RSC Advances

PAPER

View Article Online
View Journal | View Issue

Cite this: *RSC Adv.*, 2019, **9**, 23316

An aggregation-induced emission-based fluorescence turn-on probe for Hg^{2+} and its application to detect Hg^{2+} in food samples†

Lijun Tang, *[a] Haili Yu,[a] Keli Zhong,[a] Xue Gao[b] and Jianrong Li *[b]

Received 13th June 2019
Accepted 22nd July 2019

DOI: 10.1039/c9ra04440j

rsc.li/rsc-advances

In this work, we presented a new tetraphenylethene-derived fluorescent probe **TPE-M** for Hg^{2+} detection in an aqueous solution. Probe **TPE-M** is molecularly dissolved in CH_3OH/PBS (20 mM, pH = 7.4) (3 : 7, v/v) mixed solution and is almost non-emissive. Reaction of **TPE-M** with Hg^{2+} leads to release of an AIE-active precursor **4**, and results in a significant fluorescence enhancement. The Hg^{2+} recognition process has some distinct advantages including rapid response, high selectivity and sensitivity, strong anti-interference ability, and a low detection limit (4.16×10^{-6} M). Moreover, the probe is applicable to detect Hg^{2+} in real food samples such as shrimp, crab and teas, suggesting the practical applicability of **TPE-M**.

Introduction

Mercury ion (Hg^{2+}), as a notorious toxic heavy metal ion, possesses significant influence on human health by accumulating in the body along with the skin, respiratory tract and food chain.[1] Hg^{2+} accumulation in the food chain is harmful to DNA and the central nervous system.[2,3] Therefore, effective detection of Hg^{2+} is of great significance.

So far, several effective methods for Hg^{2+} detection, including liquid chromatography (LC),[4] atomic absorption spectrometry (AAS),[5] atomic fluorescence spectrometry (AFS),[6] and inductively coupled plasma-mass spectrometry (ICP-MS)[7] have been established. However, these methods usually require expensive instruments, complicated sample preparations, tedious detection processes, and relatively professional operation techniques. Compared with the aforementioned methods, fluorescence techniques have received considerable attention due to their advantages such as simple operation, rapid response, high selectivity and sensitivity.[8–12] During the past few decades, a large number of Hg^{2+} selective fluorescent probes have been documented.[13–18] There are mainly two strategies for the design of fluorescent Hg^{2+} probes. One design method is based on Hg^{2+}-chelation induced fluorescence changes of the probe,[19–21] however, some probes based on this strategy are prone to suffer from the interference of other metal ions (Cu^{2+}, Co^{2+}, Fe^{2+}, and Pb^{2+}),[22–25] or fluorescence quenching due to the heavy atom effect induced by the Hg^{2+} ion.[26–29] Another methodology is based on Hg^{2+}-triggered specific reaction of the probe.[30–34] Compared with the chelation method, the specific chemical reactions triggered by Hg^{2+} can lead to unique spectral changes in fluorescence or absorbance, which makes the probes more advantageous in terms of selectivity and sensitivity. Whereas, the latter protocol sometimes may be affected by the aggregation-caused quenching (ACQ) effect of the reaction product with hydrophobic nature.[35,36] The discovery of aggregation-induced emission (AIE) phenomenon[37] provides an opportunity to address this limitation. Although there are some fluorescent Hg^{2+} probes based on AIE mechanism have been documented,[24,38–45] development of new AIE-based fluorescent Hg^{2+} probes with high selectivity and rapid response is still highly desirable.

Tetraphenylethene (TPE) is a well-known AIE-active luminogen, and a great number of TPE-based derivatives with distinct AIE properties have been established. However, the TPE aggregates have shorter emission wavelengths, and TPE-based fluorescent Hg^{2+} probes are still rare. One can envision that by extending the conjugation structure and incorporate a dithioacetal group on a TPE-based fluorogen, a new Hg^{2+} selective fluorescent probe with red-shifted emission based on AIE mechanism can be obtained. We herein synthesized a new TPE-derived Hg^{2+} selective fluorescent probe **TPE-M** by condensation of TPE-derived aldehyde **4** and 3-mercaptopropionic acid (Scheme 1). It is surmised that the Hg^{2+}-triggered hydrolysis of dithioacetal in **TPE-M** will release its precursor **4**, a potentially AIE-active compound, and thus can realize Hg^{2+} detection in an aqueous medium. The carboxylic acid-containing dithioacetal moiety doped in probe **TPE-M** can

[a]*College of Chemistry and Chemical Engineering, Bohai University, Jinzhou, 121013, China. E-mail: ljtang@bhu.edu.cn*

[b]*College of Food Science and Technology, Bohai University, National & Local Joint Engineering Research Center of Storage, Processing and Safety Control Technology for Fresh Agricultural and Aquatic Products, The Fresh Food Storage and Processing Technology Research Institute of Liaoning Provincial Universities, Jinzhou, 121013, China. E-mail: lijr6491@163.com*

† Electronic supplementary information (ESI) available. See DOI: 10.1039/c9ra04440j

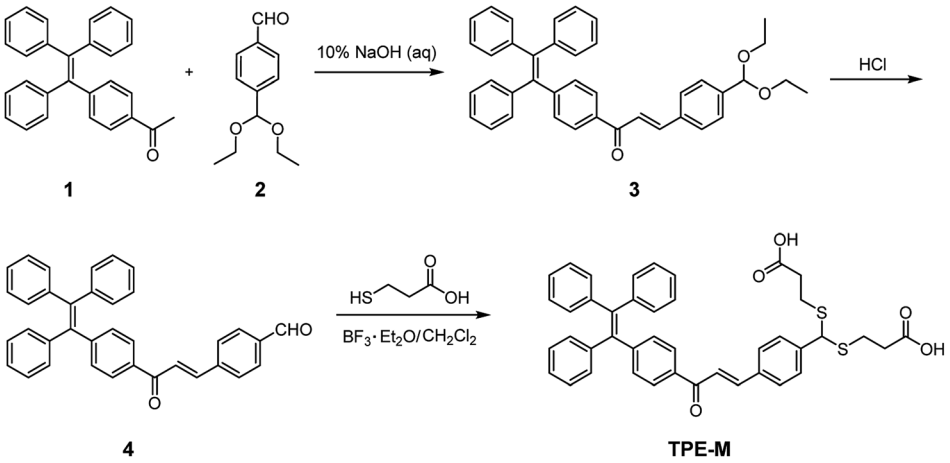

Scheme 1 Synthesis of probe TPE-M.

provide Hg^{2+} recognition site and enable good solubility of **TPE-M** in aqueous solution. Further studies demonstrate that probe **TPE-M** can detect Hg^{2+} in CH_3OH/PBS mixed solvent based on AIE mechanism.

Experimental section

Materials and instruments

Unless otherwise specified, solvents and reagents were of analytical grade from commercial suppliers and used directly. Compound **1** (ref. 46) was synthesized according to literature method. ^{1}H NMR and ^{13}C NMR spectra were measured on an Agilent 400-MR spectrometer. High resolution mass spectroscopy (HRMS) was recorded on an Agilent 1200 time-of-flight mass spectrometer (Bruker, microTOF-Q). Fluorescence measurements were performed on a Sanco 970-CRT spectrofluorometer (Shanghai, China). Dynamic light scattering (DLS) experiments were performed with a Malvern Zetasizer Nano-ZS90 DLS system (Malvern Instruments Ltd., Worcestershire, UK).

General procedure for spectroscopic analysis

Double distilled water was used throughout the experiments. Probe **TPE-M** was dissolved in CH_3OH/PBS (20 mM, pH = 7.4) (3 : 7, v/v) to afford the test solution (10 μM). Titration experiments were performed in 10 mm quartz cuvettes at 25 °C. Metal ions (as chloride or nitrate salts, 10 mM) were added to the host solution and used for the titration experiment.

Synthesis

Synthesis of compound 3. Compounds **1** (1.87 g, 5 mmol) and **2** (901 mg, 5 mmol) were dissolved in 10% NaOH (2 mL) in ethanol and stirred at room temperature for 24 h. After filtration, the solvent was evaporated under reduced pressure, and the crude product was purified by silica column chromatography (ethyl acetate/petroleum ether = 1 : 30, v/v) to give **3** as a yellow solid (1.35 g, yield 48%). Mp 49.9–51.8 °C. ^{1}H NMR (400 MHz, DMSO-d_6) δ 7.94 (d, J = 8.0 Hz, 2H), 7.90–7.85 (m, 3H), 7.70 (d, J = 15.6 Hz, 1H), 7.45 (d, J = 8.4 Hz, 2H), 7.18–7.12 (m, 11H), 7.02–6.98 (m, 6H), 5.52 (s, 1H), 3.59–3.45 (m, 4H), 1.15 (t, J = 7.0 Hz, 6H); ^{13}C NMR (100 MHz, DMSO-d_6) δ 188.7, 148.7, 143.8, 143.2, 143.0, 142.5, 142.0, 140.1, 135.8, 135.0, 131.5, 131.1, 131.0, 129.1, 128.6, 128.4, 128.3, 127.4, 127.3, 122.4, 100.9, 61.3, 15.6. HRMS (ESI+): calcd for $C_{40}H_{37}O_3$ $[M + H]^+$, 565.2743; found: 565.2972.

Synthesis of compound 4. To a solution of compound **3** (1.25 g, 2.21 mmol) in 30 mL ethanol, 2 mL of hydrochloric acid (1 M) was added at room temperature, and the reactant was further stirred for 2 h. The precipitates formed were collected by filtration and the filtrate was evaporated to dryness under reduced pressure. The residue was dissolved in CH_2Cl_2 and washed with water, the organic layer was dried over anhydrous Na_2SO_4. After filtration and removing the solvent under reduced pressure, the residue was combined with the collected precipitates, and the crude product was purified by silica gel column chromatography (ethyl acetate/petroleum ether = 1 : 20, v/v) to obtain **4** as pale yellow solids (890.47 mg, yield 82%). Mp 206.7–207.8 °C. ^{1}H NMR (400 MHz, DMSO-d_6) δ 10.04 (s, 1H), 8.09 (d, J = 8.0 Hz, 2H), 8.05 (d, J = 15.6 Hz, 1H), 7.98–7.95 (m, 4H), 7.76 (d, J = 15.6 Hz, 1H), 7.19–7.12 (m, 11H), 7.03–6.99 (m, 6H); ^{13}C NMR (100 MHz, DMSO-d_6) δ 193.1, 188.6, 149.0, 143.2, 143.1, 143.0, 142.5, 140.7, 140.1, 137.4, 135.5, 131.6, 131.1, 131.0, 130.3, 129.9, 128.7, 128.4, 128.3, 127.4, 127.3, 125.2. HRMS (ESI−): calcd for $C_{36}H_{29}O_4$ $[M + 2H_2O–H]^-$, 525.2066; found: 525.1789.

Synthesis of probe TPE-M. To an ice-cooled solution of compound **4** (800 mg, 1.63 mmol) in anhydrous dichloromethane (13 mL) under nitrogen atmosphere, a solution of 3-mercaptopropionic acid (259.5 mg, 2.45 mmol) and BF_3–Et_2O (1 mL) in 5 mL DMF was added dropwise, and the reaction mixture was stirred at room temperature for 12 h. After that, the reaction mixture was concentrated and extracted with ethyl acetate. The combined organic layer was successively washed with 1.0 M HCl and brine and dried over anhydrous Na_2SO_4. After removing the solvent under reduced pressure, the residue was purified by silica column chromatography (MeOH/DCM = 1 : 30, v/v) to obtain **TPE-M** as orange yellow solid (547.23 mg, yield 49%). Mp

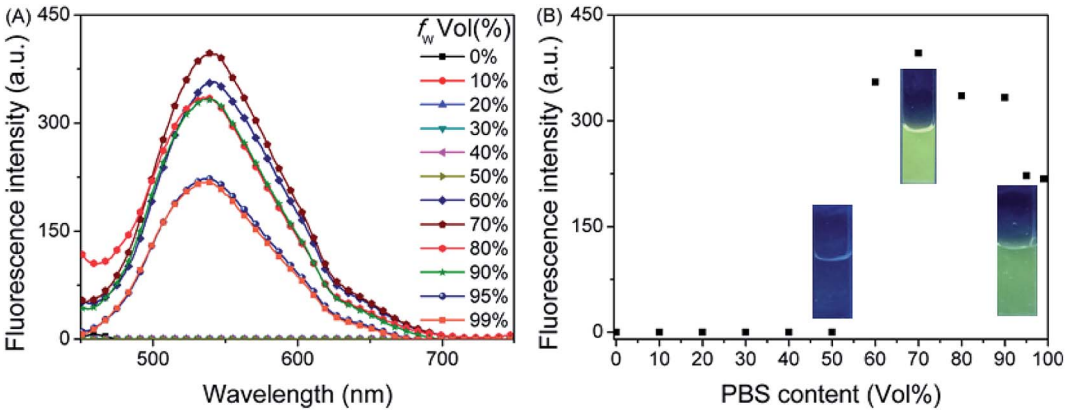

Fig. 1 (A) Fluorescence spectrum of **4** (10 μM) in CH_3OH/PBS (20 mM, pH = 7.4) with different PBS content; (B) changes in fluorescence intensity (537 nm) of **4** in CH_3OH/PBS (20 mM, pH = 7.4) with different PBS content.

74.1–75.2 °C. ^{1}H NMR (400 MHz, DMSO-d_6) δ 12.32 (br, 2H), 7.94 (d, J = 8.0 Hz, 2H), 7.90–7.85 (m, 3H), 7.69 (d, J = 15.2 Hz, 1H), 7.49 (d, J = 8.4 Hz, 2H), 7.16–7.14 (m, 11H), 7.03–6.99 (m, 6H), 5.32 (s, 1H), 2.78–2.71 (m, 2H), 2.67–2.61 (m, 2H) (proton signals for two CH_2 groups are overlapped with the peak of residue DMSO); ^{13}C NMR (100 MHz, DMSO-d_6) δ 188.6, 173.3, 148.7, 143.6, 143.2, 143.0, 142.5, 140.1, 135.8, 134.6, 131.5, 131.1, 131.0, 129.6, 128.6, 128.4, 128.3, 127.4, 127.3, 122.5, 51.9, 34.5, 27.5. HRMS (ESI+): calcd for $C_{42}H_{36}NaO_5S_2$ $[M + Na]^+$, 707.1902; found: 707.1011.

Result and discussion

AIE properties of intermediate 4

Based on the probe design principle, namely, probe **TPE-M** undergoes Hg^{2+}-triggered hydrolysis to release AIE-active compound **4**, the AIE characteristic of compound **4** was firstly examined. The changes in fluorescence behavior of **4** was examined in a mixed solvent of CH_3OH/PBS (20 mM, pH = 7.4) with different PBS contents (f_w) (Fig. 1). Compound **4** is non-emissive when f_w ranging from 0 to 50%. On further increase f_w to 60–70%, a greatly enhanced emission band centered at 537 nm can be observed. Further increase of f_w leads to partial fluorescence quenching. When illuminate the solution of **4** in CH_3OH/PBS (20 mM, pH = 7.4) (3 : 7, v/v) with a laser pointer, an obvious light path can be observed (Fig. S1†), indicating that compound **4** form aggregates. Dynamic light scattering (DLS) measurements showed an average particle size of 412 nm in diameter (Fig. S2†), indicating the formation of nano-aggregates of compound **4**.

Fluorescence recognition of TPE-M to Hg^{2+}

Promoted by the AIE property of compound **4**, we then explored the response of probe **TPE-M** toward Hg^{2+} ions in CH_3OH/PBS (20 mM, pH = 7.4) (3 : 7, v/v). In order to examine the solubility of **TPE-M** in the mixed solvent, the relationship between absorbance and probe concentration ranging from 4 to 14 μM was first investigated (Fig. S3†). The results provide a good linear relationship (R^2 > 0.99) between absorbance and probe concentration, demonstrating that all probes are molecularly dissolved. Then we detected the fluorescence response of probe **TPE-M** (10 μM) to different concentrations of Hg^{2+}. As shown in Fig. 2, a gradually enhanced fluorescence emission band centered at 538 nm was observed upon stepwise addition of Hg^{2+} to the probe solution, and the fluorescence intensity leveled off after 1.5 equiv. of Hg^{2+} was used. The observed emission wavelength is quite similar to that of **4** in CH_3OH/PBS (20 mM, pH = 7.4) (3 : 7, v/v), suggesting the formation of aggregates of **4**. DLS analysis of the Hg^{2+}-treated **TPE-M** solution revealed the formation of aggregates with an average particle size of 419 nm (Fig. S4†), which is in good agreement with the DLS data of compound **4** solution. The titration results indicate that probe **TPE-M** has good sensing characteristics for Hg^{2+}. Based on the titration curve, a satisfactory linear relationship (R^2 > 0.99) was obtained between the emission intensity (at 538 nm) and Hg^{2+} concentration (0 to 15 μM) (Fig. S5†). The detection limit of probe **TPE-M** for Hg^{2+} was estimated to be 4.157×10^{-6} M on the basis of signal to noise method (LOD = $3\sigma/k$, σ is the standard deviation of the blank solution; k is the slope of the calibration curve). Time-course study shows that the response of probe **TPE-M** to Hg^{2+} (1.5 equiv.) is rapid and can be completed within 4 seconds (Fig. 3). The pseudo first-order

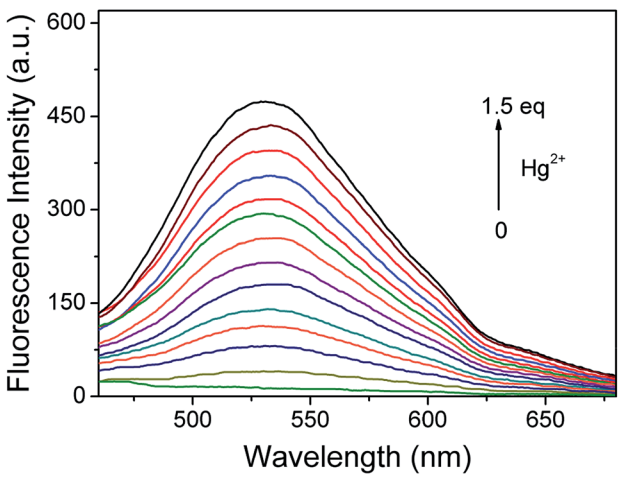

Fig. 2 Changes of fluorescence spectrum of probe **TPE-M** (10 μM) in CH_3OH/PBS (20 mM, pH = 7.4) (3 : 7, v/v) on incremental addition of Hg^{2+} (0–15 μM). λ_{ex} = 395 nm.

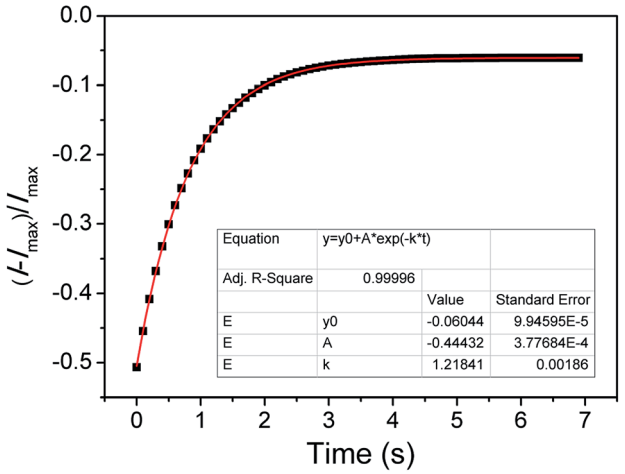

Fig. 3 Reaction kinetic study of TPE-M with Hg^{2+} under pseudo first-order conditions.

reaction rate constant k is calculated to be 1.218 s^{-1} according to the equation $I_t = I_{max} + A \times \exp(-k \times t)$ (I_t is the emission intensity at 538 nm at time t, and I_{max} is the maximum emission intensity at 538 nm),[47] indicating that probe **TPE-M** has potential real-time detection capability for Hg^{2+} ions.

In order to further confirm the selectivity of probe **TPE-M** to Hg^{2+}, the fluorescence spectra of probe **TPE-M** in the presence of different metal ions (including Cu^{2+}, Co^{2+}, Zn^{2+}, Cd^{2+}, Cr^{3+}, Fe^{3+}, Sr^{2+}, Na^{+}, Hg^{2+}, Ag^{+}, Pb^{2+}, Mn^{2+}, Al^{3+}, K^{+}, Ni^{2+}, Ba^{2+}, Mg^{2+}, Fe^{2+} and Ca^{2+}, 1.5 equiv. for each metal ion) were subsequently explored (Fig. 4). Except for Hg^{2+}, other tested metal ions caused a minor or negligible fluorescence enhancement. It is noteworthy that addition of Ag^{+} or Pb^{2+} also elicits a slight fluorescence enhancement at 538 nm. The Ag^{+}-induced fluorescence enhancement can be attributed to the Ag^{+}-triggered hydrolysis of probe **TPE-M**, which is similar to our previous result.[44] Since

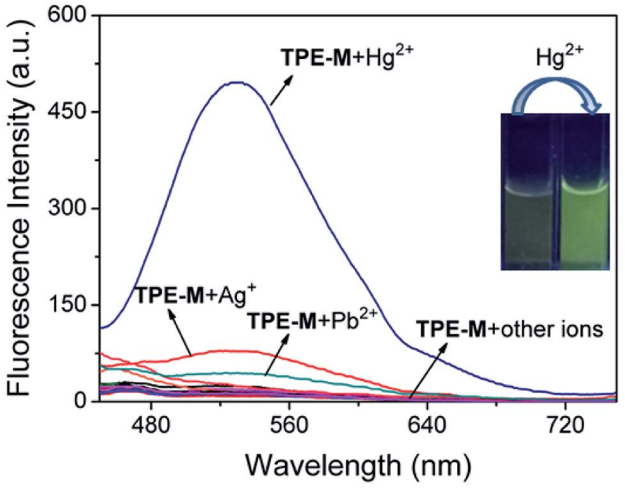

Fig. 4 Fluorescence spectrum of probe TPE-M (10 μM) in CH_3OH/PBS (20 mM, pH = 7.4) (3 : 7, v/v) in the presence of 1.5 equiv. of various metal ions. λ_{ex} = 395 nm. Inset: fluorescence color changes of probe TPE-M before and after addition of Hg^{2+}.

Ag^{+} and Cl^{-} are prone to form insoluble AgCl, no Ag^{+} ion at the micromole level can be found under physiological conditions (containing Cl^{-} ions at the millimole level). The Pb^{2+}-induced emission enhancement is most likely due to the Pb^{2+}-triggered hydrolysis of **TPE-M** because of the sulfophilic property of Pb^{2+} ions.[48,49] Whereas, compared with the effect of Hg^{2+}, the emission enhancement induced by Ag^{+} and Pb^{2+} are very weak. Therefore, the results suggest that probe **TPE-M** has excellent selectivity for Hg^{2+} over other tested metal ions.

To get insight into the practical applicability of probe **TPE-M**, competitive experiments were them performed (Fig. 5). As shown in the Fig. 5, other coexisting metal ions did not significantly interfere with the recognition of Hg^{2+}. We also investigated the effect of pH on the fluorescence intensity changes of **TPE-M** with and without Hg^{2+} (Fig. 6). Under alkaline conditions, significant fluorescence quenching of **TPE-M** + Hg^{2+} was observed, which may attributed to the generation of mercuric

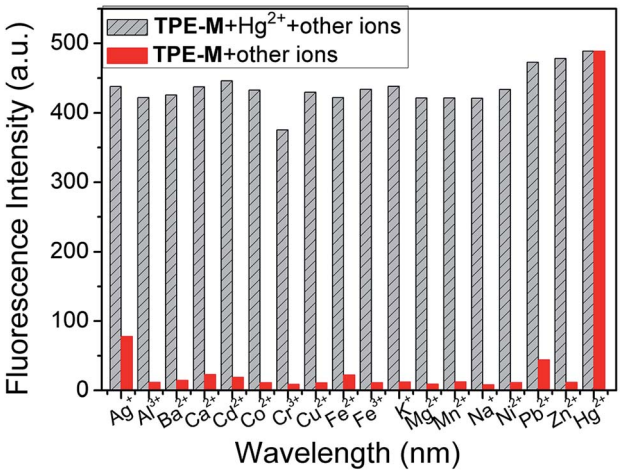

Fig. 5 Change in fluorescence intensity of probe TPE-M (10 μM) in the presence of different metal ions (red bars) and further addition of Hg^{2+} (gray stripe). Metal ions were used as 15 μM.

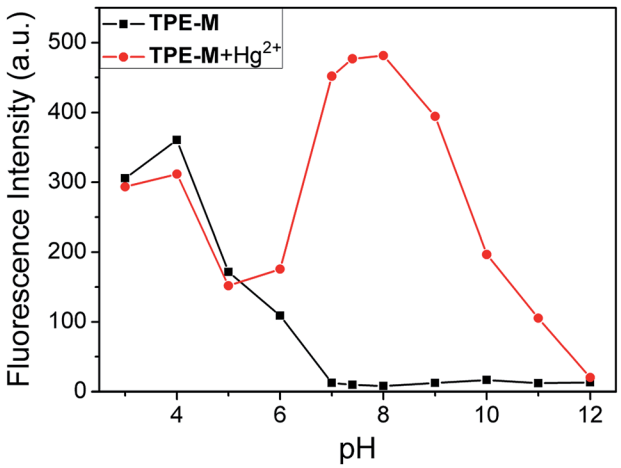

Fig. 6 Fluorescence intensity changes of probe TPE-M in the presence and absence of Hg^{2+} under different pH conditions.

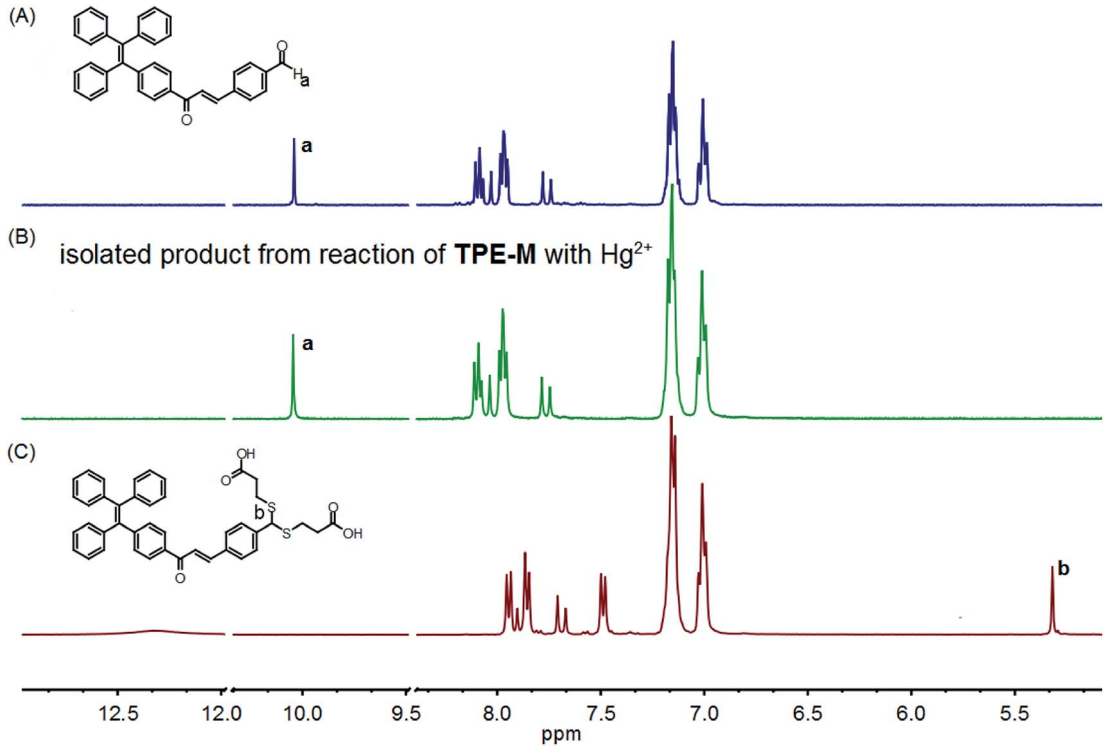

Fig. 7 Comparison of partial ^{1}H NMR spectra of compound **4** (A), isolated product from reaction of **TPE-M** with Hg^{2+} (B), and **TPE-M** (C) in DMSO-d_6.

oxide coming from the reaction between OH^- and Hg^{2+},[50] this reaction prevented the Hg^{2+}-triggered hydrolysis of dithioacetal group in the probe. The results show that probe **TPE-M** is suitable to detect Hg^{2+} under near neutral and weak alkaline conditions with pH range from 7.0 to 9.0.

Detection mechanism of TPE-M for Hg^{2+}

To verify the proposed Hg^{2+}-triggered hydrolysis of probe **TPE-M** to release compound **4**, an additional reaction of **TPE-M** with Hg^{2+} was conducted, and the ^{1}H NMR spectrum of the separated product was compared with that of **4** (Fig. 7). The methine proton (H_b) signal of the dithioacetal moiety in **TPE-M** appeared at 5.31 ppm (Fig. 7C), this signal disappeared in the separated product (Fig. 7B). Concomitantly, a new proton signal appearing at 10.04 ppm (Fig. 7B) was observed, which is assignable to the aldehyde proton (H_a) of compound **4**, and the aromatic proton signals (Fig. 7B) have a pattern similar to that compound **4** (Fig. 7A). The almost identical ^{1}H NMR spectra of the separated product and **4** demonstrate that reaction of **TPE-M** with Hg^{2+} indeed releasing **4**. Another conclusive evidence for the formation of compound **4** was from the HRMS analysis of probe **TPE-M** + Hg^{2+} solution (Fig. S6†). The peak appearing at m/z = 713.4981 can be assigned to the species of $[\mathbf{4} + 7CH_3OH–H]^-$ (calcd m/z = 713.3695), indicating the formation of compound **4**. These results indicate that probe **TPE-M** is transformed into **4** on interaction with adding Hg^{2+} ions. The released AIE-active compound **4** aggregates in the detection medium, which is the reason for the observed fluorescence. The detection mechanism of probe **TPE-M** for Hg^{2+} is shown in Scheme 2.

Application of TPE-M for Hg^{2+} detection in real samples

To further explore the potential applicability of **TPE-M**, we examined its utility for Hg^{2+} detection in some food samples including crabs, shrimps and teas. Firstly, the pretreated

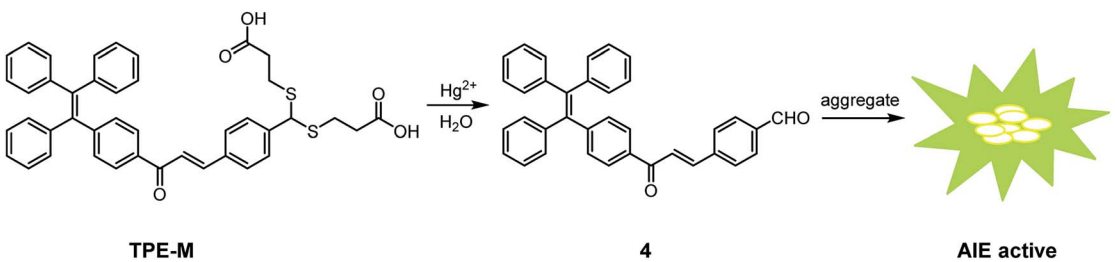

Scheme 2 Detection mechanism of probe TPE-M for Hg^{2+}.

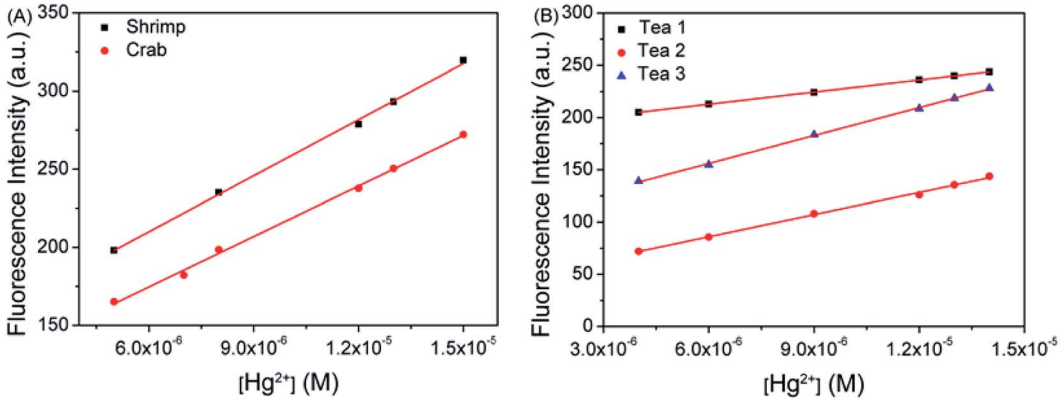

Fig. 8 Detection of Hg^{2+} in crab and shrimp (A) and tea (B) samples by probe **TPE-M**.

Table 1 Application of **TPE-M** in determination of Hg^{2+} in seafood samples

Sample	Added (μM)	Detect (μM)	RSD (%)	Recovery (%)	Relative error (%)
Shrimp	5.0	4.67	1.45	93.47	6.53
	8.0	8.43	0.71	105.40	5.40
	15.0	14.53	2.00	96.85	3.15
Crab	5.0	5.20	1.20	104.10	4.10
	8.0	7.95	1.26	99.32	0.68
	15.0	15.33	1.52	102.20	2.20

Table 2 Application of **TPE-M** in determination of Hg^{2+} in tea samples

Sample	Added (μM)	Detect (μM)	RSD (%)	Recovery (%)	Relative error (%)
Tea 1	6.0	6.02	0.16	100.41	0.41
	9.0	8.59	0.27	95.44	4.56
	14.0	14.64	0.71	104.54	4.54
Tea 2	6.0	6.19	1.17	103.16	3.16
	9.0	8.95	0.50	99.49	0.51
	14.0	14.49	0.09	103.47	3.47
Tea 3	6.0	6.56	0.80	109.35	9.35
	9.0	9.46	1.78	105.08	5.08
	14.0	14.16	0.62	101.10	1.15

shrimp or crab sample solution (the detailed procedures for sample pretreatment are described in ESI†) was mixed with methanol with 7 : 3 volume ratio, and spiked with different concentrations of Hg^{2+}. Then 10 μM of probe **TPE-M** was added to the Hg^{2+} spiked solutions and the fluorescence spectra were measured. As shown in Fig. 8A, the fluorescence intensity of the samples displayed good linear relationships against the added Hg^{2+} concentration, and the relevant calculations are shown in Table 1. It can be seen that the recoveries measured are between 93.47% and 105.4%, and the relative standard deviations (RSDs) are less than 2%, and the relative errors are less than 6.53%. The addition amount of Hg^{2+} and the measured value reach a good consistency, indicating that the analysis of Hg^{2+} in the seafood samples is reliable and feasible.

Subsequently, each tea sample was mixed with methanol at 7 : 3 volume ratios, and different concentrations of Hg^{2+} were added thereto, and then detected by probe **TPE-M**. As shown in Fig. 8B, the fluorescence intensity of the probe in the real sample showed good linear relationships *versus* the spiked Hg^{2+} concentration, and the relevant calculations are shown in Table 2. The results show that the measured recoveries are between 95.44% and 109.35%, the relative standard deviations (RSDs) are less than 1.78%, and the relative errors are less than 9.35%. These results demonstrate that probe **TPE-M** can be used to detect Hg^{2+} in real tea samples.

Conclusion

In summary, we reported a new tetraphenylethene-derived fluorescent probe **TPE-M** for Hg^{2+} detection in CH_3OH/PBS (20 mM, pH = 7.4) (3 : 7, v/v) solution. On treatment of non-emissive probe **TPE-M** solution with Hg^{2+}, an AIE-active

compound **4** is released and elicits a noticeable fluorescence enhancement. The Hg^{2+} recognition event holds the advantages of rapid response, high selectivity and sensitivity, strong anti-interference ability, and a low detection limit. In addition, **TPE-M** can be applied to detect Hg^{2+} in real food samples including shrimp, crab and teas, advocating the practical applicability of **TPE-M**.

Conflicts of interest

There are no conflicts to declare.

Acknowledgements

The project was supported by the National Natural Science Foundation of China (No. 21878023, U1608222 and 21304009), the LiaoNing Revitalization Talents Program, the Natural Science Foundation of Liaoning Province (20170540019), and the Doctoral Scientific Research Foundation of Liaoning Province (No. 20170520416).

Notes and references

1 C. O. R. Okpala, G. Sardo, S. Vitale, G. Bono and A. Arukwe, *Crit. Rev. Food Sci. Nutr.*, 2018, **58**, 1986–2001.
2 P. Grandjean, P. Weihe, R. F. White and F. Debes, *Environ. Res.*, 1998, **77**, 165–172.
3 T. Takeuchi, N. Morikawa, H. Atsumoto and Y. Shiraishi, *Acta Neuropathol.*, 1962, **2**, 40–57.
4 M. Wang, W. Feng, J. Shi, F. Zhang, B. Wang, M. Zhu, B. Li, Y. Zhao and Z. Chai, *Talanta*, 2007, **71**, 2034–2039.
5 M. Filippelli, *Anal. Chem.*, 1987, **59**, 116–118.
6 T. Labatzke and G. Schlemmer, *Anal. Bioanal. Chem.*, 2004, **378**, 1075–1082.
7 H. Chen, J. Chen, X. Jin and D. Wei, *J. Hazard. Mater.*, 2009, **172**, 1282–1287.
8 D. T. Quang and J. S. Kim, *Chem. Rev.*, 2010, **110**, 6280–6301.
9 H. Zhu, J. Fan, B. Wang and X. Peng, *Chem. Soc. Rev.*, 2015, **44**, 4337–4366.
10 L. Tang, M. Tian, H. Chen, X. Yan, K. Zhong and Y. Bian, *Dyes Pigm.*, 2018, **158**, 482–489.
11 L. Tang, P. He, X. Yan, J. Sun, K. Zhong, S. Hou and Y. Bian, *Sens. Actuators, B*, 2017, **247**, 421–427.
12 Q. Hu, W. Li, C. Qin, L. Zeng and J. T. Hou, *J. Agric. Food Chem.*, 2018, **66**, 10913–10920.
13 L. Tang, F. Li, M. Liu and R. Nandhakumar, *Spectrochim. Acta, Part A*, 2011, **78**, 1168–1172.
14 P. Mahato, S. Saha, P. Das, H. Agarwalla and A. Das, *RSC Adv.*, 2014, **4**, 36140–36174.
15 M. J. Culzoni, A. Muñoz de la Peña, A. Machuca, H. C. Goicoechea and R. Babiano, *Anal. Methods*, 2013, **5**, 30–49.
16 N. Kumar, V. Bhalla and M. Kumar, *Analyst*, 2014, **139**, 543–558.
17 Y. Zhou, X. He, H. Chen, Y. Wang, S. Xiao, N. Zhang, D. Li and K. Zheng, *Sens. Actuators, B*, 2017, **247**, 626–631.
18 Y. Zhang, H. Chen, D. Chen, D. Wu, Z. Chen, J. Zhang, X. Chen, S. Liu and J. Yin, *Sens. Actuators, B*, 2016, **224**, 907–914.
19 P. Srivastava, S. S. Razi, R. Ali, R. C. Gupta, S. S. Yadav, G. Narayan and A. Misra, *Anal. Chem.*, 2014, **86**, 8693–8699.
20 S. S. Razi, R. Ali, R. C. Gupta, S. K. Dwivedi, G. Sharma, B. Koch and A. Misra, *J. Photochem. Photobiol., A*, 2016, **324**, 106–116.
21 P. Srivastava, M. Shahid and A. Misra, *Org. Biomol. Chem.*, 2011, **9**, 5051–5055.
22 I. Kim, N. E. Lee, Y. J. Jeong, Y. H. Chung, B. K. Cho and E. Lee, *Chem. Commun.*, 2014, **50**, 14006–14009.
23 L. Zong, C. Wang, Y. Song, Y. Xie, P. Zhang, Q. Peng, Q. Li and Z. Li, *Sens. Actuators, B*, 2017, **252**, 1105–1111.
24 W. Fang, G. Zhang, J. Chen, L. Kong, L. Yang, H. Bi and J. Yang, *Sens. Actuators, B*, 2016, **229**, 338–346.
25 A. Aliberti, P. Vaiano, A. Caporale, M. Consales, M. Ruvo and A. Cusano, *Sens. Actuators, B*, 2017, **247**, 727–735.
26 K. Zhong, X. Zhou, R. Hou, P. Zhou, S. Hou, Y. Bian, G. Zhang, L. Tang and X. Shang, *RSC Adv.*, 2014, **4**, 16612–16617.
27 Z. Wu, Y. Zhang, J. S. Ma and G. Yang, *Inorg. Chem.*, 2006, **45**, 3140–3142.
28 B. K. Rani and S. A. John, *J. Hazard. Mater.*, 2018, **343**, 98–106.
29 S.-Y. Moon, N. J. Youn, S. M. Park and S.-K. Chang, *J. Org. Chem.*, 2005, **70**, 2394–2397.
30 M. H. Lee, S. W. Lee, S. H. Kim, C. Kang and J. S. Kim, *Org. Lett.*, 2009, **11**, 2101–2104.
31 L. Ding, M. Wu, Y. Li, Y. Chen and J. Su, *Tetrahedron Lett.*, 2014, **55**, 4711–4715.
32 K. C. Song, J. S. Kim, S. M. Park, K.-C. Chung, S. Ahn and S.-K. Chang, *Org. Lett.*, 2006, **8**, 3413–3416.
33 S. Angupillai, J.-Y. Hwang, J.-Y. Lee, B. A. Rao and Y.-A. Son, *Sens. Actuators, B*, 2015, **214**, 101–110.
34 S. Madhu, S. Josimuddin and M. Ravikanth, *New J. Chem.*, 2014, **38**, 5551–5558.
35 Y. Gao, T. Ma, Z. Ou, W. Cai, G. Yang, Y. Li, M. Xu and Q. Li, *Talanta*, 2018, **178**, 663–669.
36 Y. Yang, R. Shen, Y.-Z. Wang, F.-Z. Qiu, Y. Feng, X.-L. Tang, D.-c. Bai, G.-L. Zhang and W.-S. Liu, *Sens. Actuators, B*, 2018, **255**, 3479–3487.
37 J. Luo, Z. Xie, J. W. Y. Lam, L. Cheng, B. Z. Tang, H. Chen, C. Qiu, H. S. Kwok, X. Zhan, Y. Liu and D. Zhu, *Chem. Commun.*, 2001, **37**, 1740–1741.
38 B. Yuan, D. X. Wang, L. N. Zhu, Y. L. Lan, M. Cheng, L. M. Zhang, J. Q. Chu, X. Z. Li and D. M. Kong, *Chem. Sci.*, 2019, **10**, 4220–4226.
39 X.-Q. Ma, Y. Wang, T.-B. Wei, L.-H. Qi, X.-M. Jiang, J.-D. Ding, W.-B. Zhu, H. Yao, Y.-M. Zhang and Q. Lin, *Dyes Pigm.*, 2019, **164**, 279–286.
40 T. Gao, X. Huang, S. Huang, J. Dong, K. Yuan, X. Feng, T. Liu, K. Yu and W. Zeng, *J. Agric. Food Chem.*, 2019, **67**, 2377–2383.
41 X. Wen and Z. Fan, *Sens. Actuators, B*, 2017, **247**, 655–663.
42 Y. Jiang, Y. Chen, M. Alrashdi, W. Luo, B. Z. Tang, J. Zhang, J. Qin and Y. Tang, *RSC Adv.*, 2016, **6**, 100318–100325.
43 S. Ozturk and S. Atilgan, *Tetrahedron Lett.*, 2014, **55**, 70–73.

44 D. Xu, L. Tang, M. Tian, P. He and X. Yan, *Tetrahedron Lett.*, 2017, **58**, 3654–3657.
45 D. D. La, S. V. Bhosale, L. A. Jones and S. V. Bhosale, *ACS Appl. Mater. Interfaces*, 2018, **10**, 12189–12216.
46 H. Gao, D. Xu, X. Liu, A. Han, L. Zhou, C. Zhang, Z. Li and J. Dang, *Dyes Pigm.*, 2017, **139**, 157–165.
47 L. Tang, D. Xu, M. Tian and X. Yan, *J. Lumin.*, 2019, **208**, 502–508.
48 H.-Q. Jin, H.-B. Liu, Y.-Y. Xie, Y.-G. Zhang, Q.-Q. Xu, L.-J. Mao, X.-J. Li, J. Chen, F.-C. Lin and C.-L. Zhang, *Symbiosis*, 2018, **74**, 89–95.
49 E. Tiffany-Castiglioni, S. Hong, Y. Qian, Y. Tang and K. C. Donnelly, *NeuroToxicology*, 2006, **27**, 835–839.
50 D. Dai, Z. Li, J. Yang, C. Wang, J.-R. Wu, Y. Wang, D. Zhang and Y.-W. Yang, *J. Am. Chem. Soc.*, 2019, **141**, 4756–4763.